A novel type of catalytic copper cluster in nitrous oxide reductase

Kieron Brown[1], Mariella Tegoni[1], Miguel Prudêncio[2], Alice S. Pereira[2], Stephane Besson[2], José J. Moura[2], Isabel Moura[2] and Christian Cambillau[1]

[1]Architecture et Fonction des Macromolécules Biologiques, UPR 9039, CNRS, 31 Chemin Joseph Aiguier, 13402 Marseille CEDEX 20, France. [2]Departamento de Química, Centro de Química Fina e Biotecnologia, Universidade Nova de Lisboa, 2825 Monte de Caparica, Portugal.

Nitrous oxide (N_2O) is a greenhouse gas, the third most significant contributor to global warming. As a key process for N_2O elimination from the biosphere, N_2O reductases catalyze the two-electron reduction of N_2O to N_2. These 2 × 65 kDa copper enzymes are thought to contain a CuA electron entry site, similar to that of cytochrome *c* oxidase, and a CuZ catalytic center. The copper anomalous signal was used to solve the crystal structure of N_2O reductase from *Pseudomonas nautica* by multiwavelength anomalous dispersion, to a resolution of 2.4 Å. The structure reveals that the CuZ center belongs to a new type of metal cluster, in which four copper ions are liganded by seven histidine residues. N_2O binds to this center via a single copper ion. The remaining copper ions might act as an electron reservoir, assuring a fast electron transfer and avoiding the formation of dead-end products.

Nitrous oxide (N_2O) originates from biomass, fuel burning and agricultural activities[1,2]. Its conversion to N_2 is performed by denitrifying bacteria, which obtain metabolic energy by using nitrogen-oxidized compounds instead of oxygen as terminal electron acceptors in anaerobic respiration. Four enzymes have been identified in this inducible pathway: nitrate reductase, nitrite reductase, nitric oxide reductase and nitrous oxide reductase, named after the substrate they transform. The expression of these enzymes is triggered by growth on nitrate or nitrite, and low oxygen pressure. N_2O reductase (N2OR) catalyzes the final step of denitrification, that is, the two-electron reduction of N_2O to N_2 (ref. 3).

A homodimeric (2 × ~65 kDa) multicopper protein, estimated to contain eight Cu ions[4], was identified in the periplasm of *Pseudomonas stutzeri*[5] and its catalytic activity toward N_2O was soon recognized[3]. The sequences of soluble N2ORs, isolated from the periplasm of bacteria[4] or identified from soil extracts[6], share a high degree of identity, suggesting common properties[4]. Their C-terminal domains (~100 residues) are homologous to the CuA domain of bovine cytochrome *c* oxidase[7] (COXII) and include a conserved sequence motif (H $(X)_{34}$ C $(X)_3$ C $(X)_3$ H $(X)_2$ M)[8] indicative of the presence of a di-copper CuA center. The same sequence motif has been reported for other heme-Cu oxidases[9] and for subunit II of *Thermus thermophilus* ba_3-type cytochrome *c* oxidase (BA3COX)[10]. Additional evidence for a CuA center came from the typical seven-line pattern detected in EPR spectra[4]. The putative role of the CuA center as the electron acceptor site was formulated by analogy to the CuA domain of COXII[11]. In contrast, the N-terminal domain (~480 residues) has no homology to other proteins of known structure. The estimated copper content[4], along with spectroscopic results[11], indicate the presence of a second Cu center, likely to be in the large N-terminal domain. This center, designated as CuZ, was assigned as the catalytic site[11], and this was later confirmed by analysis of a catalytically inactive mutant carrying approximately half the number of the copper atoms and showing only the EPR signal typical of a CuA center[12]. The structure of the CuZ center remained unknown, and its binuclear nature has been questioned because the number of electrons needed for complete reduction was twice that expected[12].

Besides the CuA cluster mentioned above, copper proteins have been reported to contain several types of centers with one, two, or three copper ions. Mononuclear copper centers include type I, with a tetragonal coordination, and type II with a pyramidal square planar penta-coordination. Binuclear type III centers are found in catechol oxidases[13], hemocyanins[14] and tyrosinases, within a conserved four-helix bundle motif[13]. In these centers, each copper ion is coordinated by three histidines that belong to a weakly conserved sequence (H-$(X)_4$-H-$(X)_{n\approx30}$-H)[13]. Trinuclear centers are formed by the association of a type II and a type III center, as occurs in ascorbate oxidase[15], in which seven of the eight histidines are bound to the three copper ions through their Nε2 atom and are sequentially coupled in four (H-X-H) motifs[15]. The structure of N2OR from *Pseudomonas nautica* 617 (Pn N2OR) reveals that the CuZ center belongs to a novel class of metal cluster with an original pattern of four Cu ions coordinated by seven histidines. This structure allows us to propose a catalytic mechanism for the reduction of N_2O to N_2.

Overall structure

Pseudomonas nautica 617 N2OR was purified under aerobic conditions, characterized, sequenced (Fig. 1*a*) and crystallized (see Methods). The structure was solved by multiple-wavelength anomalous dispersion (MAD) phasing using the copper anomalous signal, and refined to 2.4 Å resolution; the final model has good stereochemistry and an R_{work} of 21.6% (R_{free} = 25.0%). N2OR is a dimer in the crystal, as in solution, with overall dimensions (105 × 57 × 56 Å) (Fig. 1*b*). In the asymmetric unit, three dimers (3,426 residues) form the corners of the base of a trigonal pyramid (150 × 150 × 60 Å). The dimers are related by a three-fold noncrystallographic axis oriented ~30° from the c-axis. Each N2OR monomer is composed of two distinct domains formed from contiguous segments in the amino acid sequence (Fig. 1*b*): the N-terminal domain, a β-propeller, and the C-terminal domain with a cupredoxin fold.

The β-propeller catalytic domain

The N-terminal domain (residues 10–443) adopts a seven-bladed β-propeller fold (β1/1 to β4/7), homologous to other β-propeller structures (transducin, PDB entry: 1TBG; methylamine dehydrogenase, 2BBK; galactose oxidase, 1GOF; prolyl oligopeptidase, 1QFM; and clathrin heavy chain fragment, 1BPO). The CuZ center is located at one end of the pseudo-seven-fold axis of the propeller at a position similar to that of the active sites of other β-propeller structures[16,17]. Each blade is a repeat of a four-stranded, twisted, antiparallel β-sheet. The blades of the propeller (Fig.1*b*) are radially arranged around a central channel; the interactions between the faces of the sheets are predominantly hydrophobic in nature. The propeller has approximate diameter 43 Å and height 25 Å. The polypeptide chain enters the propeller at strand β2/1 and continues through each blade in order, before ultimately leaving the domain at the C-terminus of strand β1/1. Thus, the closure of the propeller is achieved in blade 1, with the same 'Velcro snap' as previously reported in propellers with six, seven and eight blades (ref. 18 and references therein). The internal solvent channel of N2OR is conical in shape, with a 9 Å ring opening at the bottom of the propeller compared with a 22 Å opening at the top (following the

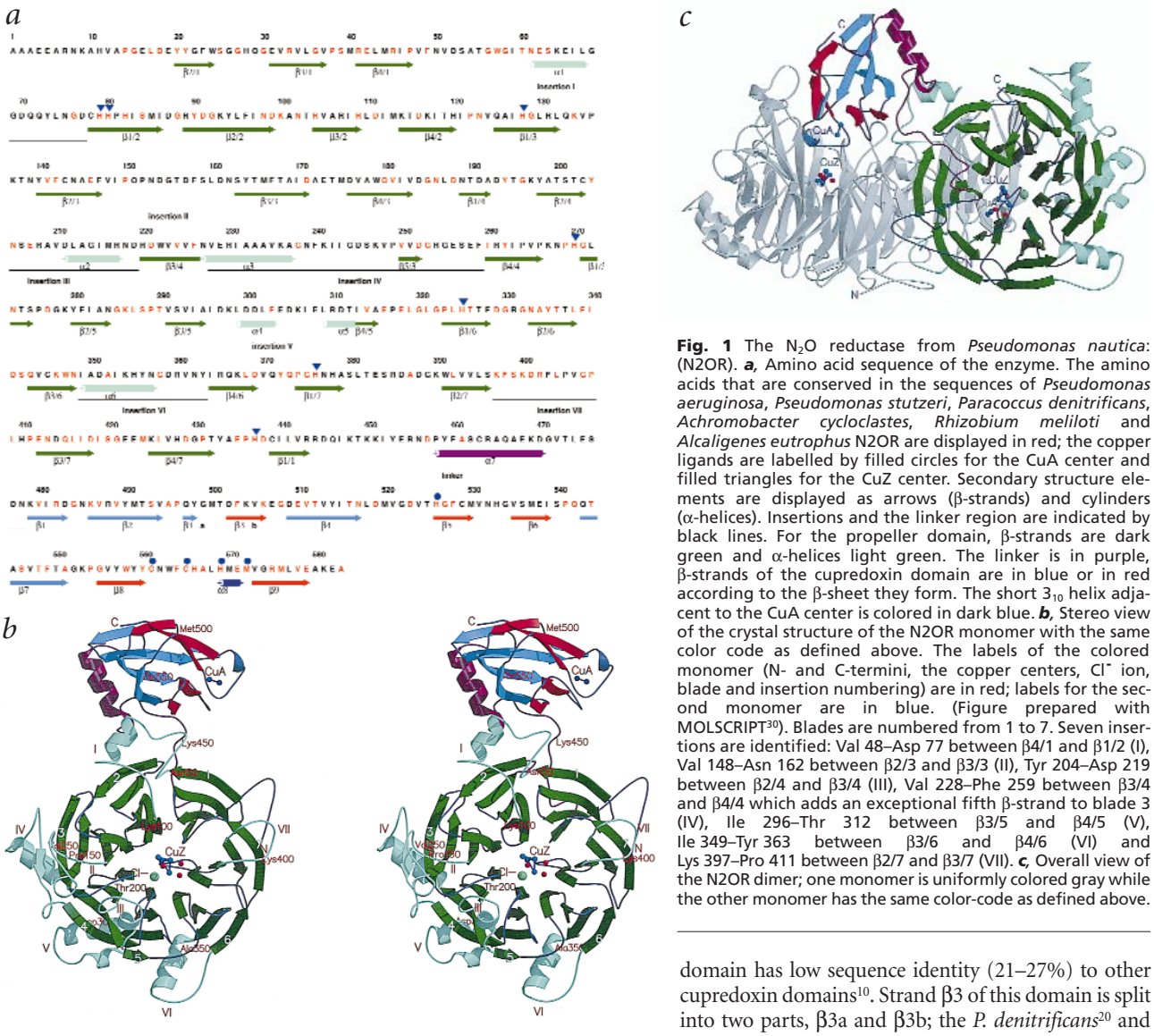

Fig. 1 The N_2O reductase from *Pseudomonas nautica*: (N2OR). ***a***, Amino acid sequence of the enzyme. The amino acids that are conserved in the sequences of *Pseudomonas aeruginosa*, *Pseudomonas stutzeri*, *Paracoccus denitrificans*, *Achromobacter cycloclastes*, *Rhizobium meliloti* and *Alcaligenes eutrophus* N2OR are displayed in red; the copper ligands are labelled by filled circles for the CuA center and filled triangles for the CuZ center. Secondary structure elements are displayed as arrows (β-strands) and cylinders (α-helices). Insertions and the linker region are indicated by black lines. For the propeller domain, β-strands are dark green and α-helices light green. The linker is in purple, β-strands of the cupredoxin domain are in blue or in red according to the β-sheet they form. The short 3_{10} helix adjacent to the CuA center is colored in dark blue. ***b***, Stereo view of the crystal structure of the N2OR monomer with the same color code as defined above. The labels of the colored monomer (N- and C-termini, the copper centers, Cl^- ion, blade and insertion numbering) are in red; labels for the second monomer are in blue. (Figure prepared with MOLSCRIPT[30]). Blades are numbered from 1 to 7. Seven insertions are identified: Val 48–Asp 77 between β4/1 and β1/2 (I), Val 148–Asn 162 between β2/3 and β3/3 (II), Tyr 204–Asp 219 between β2/4 and β3/4 (III), Val 228–Phe 259 between β3/4 and β4/4 which adds an exceptional fifth β-strand to blade 3 (IV), Ile 296–Thr 312 between β3/5 and β4/5 (V), Ile 349–Tyr 363 between β3/6 and β4/6 (VI) and Lys 397–Pro 411 between β2/7 and β3/7 (VII). ***c***, Overall view of the N2OR dimer; one monomer is uniformly colored gray while the other monomer has the same color-code as defined above.

established convention, the top of the propeller is the face where the outer β-strand (β4/*) of one blade connects to the inner β-strand (β1/*) of the next blade). The root mean square (r.m.s.) deviations of the N2OR propeller compared to the five homologous structures mentioned above vary within 2.1–2.9 Å. These differences arise principally from the nonconserved internal radii of the propellers; otherwise the orientation and angular offset of each blade are very similar. None of these structures show sequence identity with N2OR above noise threshold (7–11%). The core regions of the seven blades of N2OR are almost exactly superimposable (0.5 Å r.m.s.). Several interstrand loops are noncanonical, however, and seven insertions can be identified (Fig. 1*b*). The location and length of these insertions distinguish N2OR from all other propeller-containing proteins. Insertions I, II, III and VII of N2OR are located on the top of the propeller, whereas insertions IV, V and VI are solvent exposed and located at the bottom.

The cupredoxin domain

The C-terminal domain of N2OR (residues 478–581) consists of nine β-strands that form an antiparallel β-sandwich in the Greek key motif and adopts a cupredoxin fold already seen in bovine[19] and *Paracoccus denitrificans*[20] COXII and in BA3COX[10]. This domain has low sequence identity (21–27%) to other cupredoxin domains[10]. Strand β3 of this domain is split into two parts, β3a and β3b; the *P. denitrificans*[20] and bovine COXII[19] structures both have insertions of ~36 residues in the loop region within this strand. The CuA domain of BA3COX[10] is unique in having a shorter turn between strands β4 and β5. The N2OR N-terminal and C-terminal domains, though linked by a stretch of 33 residues (Arg 444–Asn 478), are physically separated by one of the insertions in the propeller motif (residues 47–80, insertion I, Fig. 1*b*). In the dimer, the C-terminal domain of one monomer faces the N-terminal domain of the second monomer, reminiscent of the phenomenon of 'domain exchange'[21] (Fig.1 *c*). Insertions II, III and VII act as intermonomer latches locking the CuA domain of the partner into place via hydrogen bonds. Upon dimerization, 26% of the total surface area of each monomer is buried to a 1.6 Å radius probe.

The catalytic CuZ cluster

The CuZ center of N2OR, which is almost totally reduced according to its absorption spectrum (Fig. 4*a*), comprises 4 copper ions and 10 ligands (Fig. 2*a–c*): 7 histidine residues and 3 hydroxide ions (since the exact nature of the ligands (OH^- or H_2O) cannot be ascribed using our structure or spectroscopic results in solution, they will be quoted as hydroxide ions). Two histidine residues (His 270 and His 437) of the CuZ center belong to the loops locat-

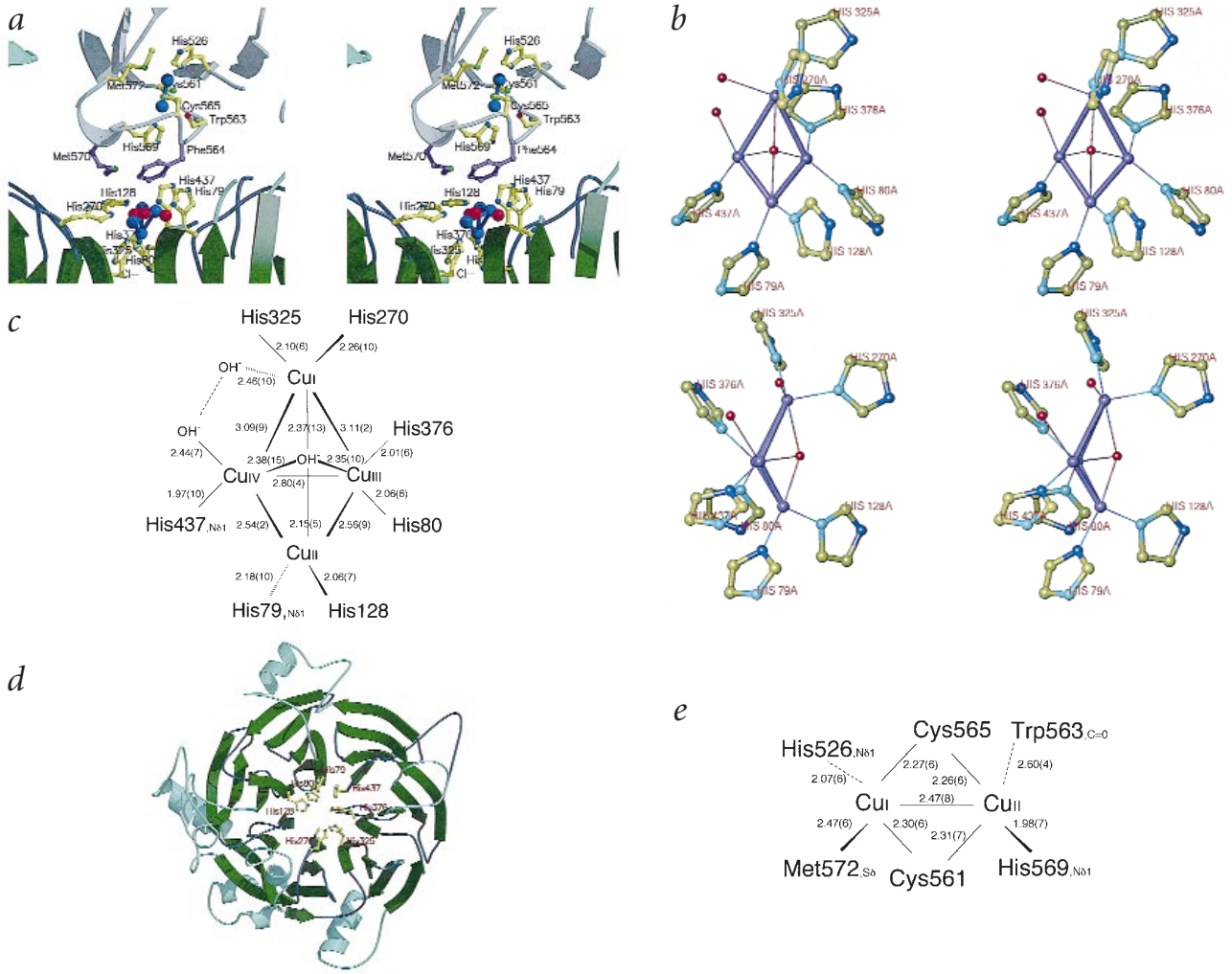

Fig. 2 The copper clusters of the N_2O reductase. ***a***, Stereo view of the interface region between the CuA center (above) and CuZ center (below). The side chains of Met 570 and Phe 564 (colored purple) from the C-terminal domain, located between the two centers, might be involved in intramolecular electron transfer. (Figure prepared with MOLSCRIPT[30]). ***b***, Stereo representation of the CuZ center; copper is in purple, OH^- in red, imidazole rings from the histidines are color atom coded, the Nδ1 being dark blue, and the Nε2 light blue. The lower view is 90° rotated with respect to the upper view. ***c***, Schematic representation of the CuZ center and its ligands (mean distances of all six molecules and errors, in parentheses, are in angstrom units). ***d***, Ribbon representation of the propeller domain with the seven histidine residues, ligands of the CuZ center. ***e***, Schematic representation of the CuA center and its ligands (mean distances of all six molecules and errors, in parentheses, are in angstrom units).

ed on the top of the propeller domain, and the remaining five (His 79, His 80, His 128, His 325, His 376) belong to the innermost strand of the blades (Fig. 2*d*). Besides these seven histidines, only one other histidine (His 82) is conserved in all N2OR sequences. The seven histidine ligands are not part of a consensus sequence; the CuZ center thus differs from other copper centers[10,13]. The CuZ center adopts the shape of a distorted tetrahedron (Fig. 2*b,c*). CuI and CuII are bound to two copper ions, whereas CuIII and CuIV are bound to three copper ions. Three copper ions have two histidine ligands; the fourth, CuIV, has only one, the second histidine being replaced by an OH^- ion. A second OH^- ion is bound to CuI, and a third is located between the four copper ions (Fig. 2*b,c*). Five histidine residues bind to the copper ions through their Nε2 atom (His 80, His 128, His 270, His 325, His 376), whereas two use their Nδ1 atoms (His 79, His 437) (Fig. 2*b,c*).

An intricate network of hydrogen bonds maintains the imidazole rings of these seven histidine residues in the appropriate orientation for coordinating the copper ions. The carboxylate group of Asp 77 stabilizes the imidazole ring of His 79, and that of Asp 188 stabilizes His 128 and His 270. His 80 Nδ1 establishes a hydrogen bond with the carbonyl group of His 128, whereas His 376 and His 437 are held in place by water molecules, themselves involved in a network of hydrogen bonds. The most original feature involves His 325, which is locked in position by a chloride ion (Fig. 2*a*), and liganded by ionic and hydrogen bonds to the guanidinium group of Arg 131, the NH main chain group of Asn 272, and the NH_2 group of Asn 273. The CuZ cluster displays approximate mirror symmetry through a plane defined by the atoms CuI and CuII, bisecting the CuIII-CuIV bond and through an orthogonal plane defined by the atoms CuIII and CuIV, bisecting the CuI-CuII bond (Fig. 2*c*). Violation of strict symmetry arises because the distances CuI-CuIII and CuI-CuIV are about 3.1 Å, whereas those of CuII-CuIII and CuII-CuIV are only about 2.5 Å. This asymmetry might arise from coordination differences between the ion pair CuI-CuII (one more OH^- ion for CuI), and the ion pair CuIII-CuIV (histidine instead of OH^- ion) or from differences in the redox state of the copper ions, since the Pn N2OR CuZ is not completely reduced.

The CuA cluster

The CuA center of N2OR is located in the loop region between

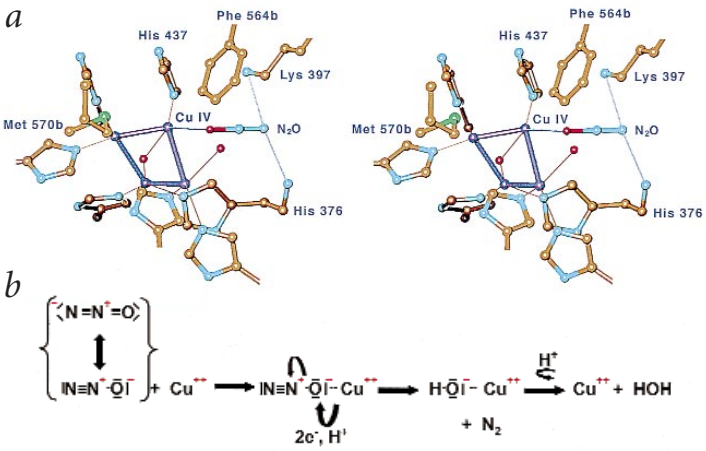

Fig. 3 Putative N_2O binding and reduction mechanism ***a***, Stereo view of a model for the binding of N_2O molecule at the CuIV of the CuZ cluster. ***b***, Putative three-step reduction mechanism of N_2O to N_2: (*i*) N_2O binds to the oxidized CuIV through its oxygen atom; (*ii*) two electrons are transferred to CuIV from the other Cu ions of the CuZ center and immediately given to the oxygen, which acquires a proton from Lys 397; concomitantly the electron pair of the N-O bond relocates on the nitrogen, liberating N_2; (*iii*) the remaining hydroxide ion could either stay on the copper, at basic pH as in our structure, or be released after protonation by a second proton from Lys 397, thus leading to the formation of a water molecule. The Cu atom represented is CuIV.

strands β8 and β9, and is adjacent to a short 3_{10}-helix (Fig. 1*a*,*b*). The CuA center is formed by two copper ions linked by the Cys 561 and Cys 565 Sγ atoms, the His 526 and His 569 Nε2 atoms, the Met 572 Sγ atom and the Trp 563 carbonyl group (Fig. 2*a*,*e*). Similar ligands have been proposed for *Achromobacter cycloclastes* N2OR by McGuirl and colleagues[22], based on sequence homology modeling using COXII[19,20] cupredoxin domain. The CuA center can be readily superimposed on the CuA centers found in COXII[19,20] and BA3COX[10] (r.m.s. deviation 1.0–1.8 Å). The two Cys Sγ atoms bind to the copper ions in a distorted square planar fashion, each Sγ interacting with both copper ions. Each histidine residue binds externally to the copper ions, whereas the Met 572 Sγ atom and the Trp 563 carbonyl group bind on opposite faces of the plane (Fig. 2*a*,*e*). As a result of the intermonomer 'domain exchange'[21], the CuA center of one monomer is in close proximity to the CuZ center of the second monomer (closest distance, 10.2 Å); two residues, Met 570 and Phe 564 from the C-terminal domain, bridge the solvent channel between the two centers, and might be involved in intramolecular electron transfer (Fig. 2*a*).

Mechanistic clues

In the N2OR CuZ center, N_2O might bind to a copper ion by either the oxygen or the nitrogen extremity. In copper nitrite reductase[23] (CuNiR), NO_2^- binds through one oxygen atom to Cu^{2+}. In contrast, the nitrogen atom is the ligand of the reduced heme of cd_1 NIR[16]. The structure of the CuZ center and the accessibility of the copper ions in the cluster suggest that the only possible site for N_2O binding is on CuIV. Removal of the OH^- ligand and two bound water molecules would leave enough space for N_2O to bind (Fig. 3*a*). Furthermore, the conserved residue Lys 397 and the NH group of His 376 would form hydrogen bonds with the external nitrogen atom of N_2O, a configuration likely to stabilize the Michaelis complex (Fig. 3*a*). Based on this observation, and in analogy with the results described with CuNiR[23], we propose a three-step reaction mechanism (Fig. 3*b*). In such a mechanism, the CuZ center would behave as an electron buffer, three copper ions being reduced by the CuA center before substrate processing. The catalytic copper would remain oxidized and therefore able to bind the substrate. Hence, this electron reservoir could favor a fast electron exchange and prevent the formation of dead-end products.

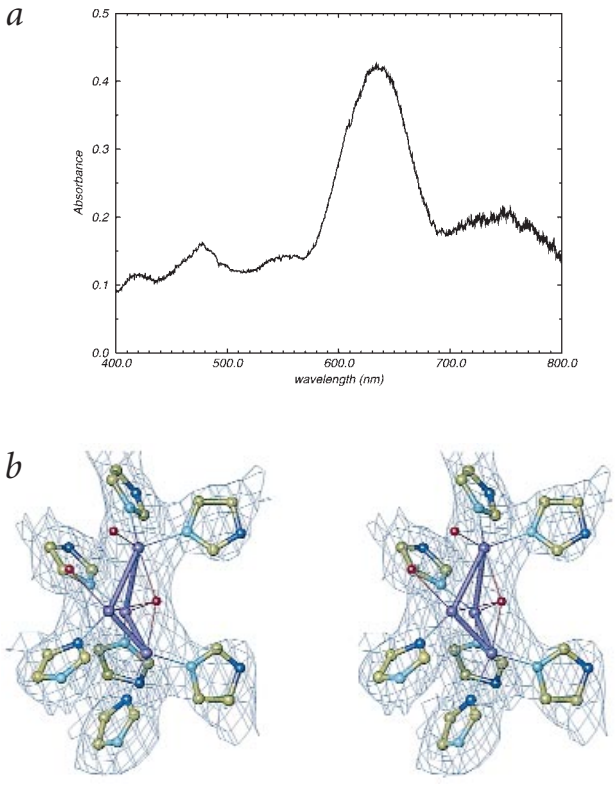

Methods

Purification, characterization and crystallization. Pn N2OR was purified under aerobic conditions and characterized by visible and EPR spectroscopy; its sequence was found to be 75% identical to that of *Pseudomonas stutzeri* N2OR. The detailed purification, characterization and sequencing procedures is presented elsewhere[31]. Briefly, Pn N2OR was isolated in two forms: a purple form and a blue form. Visible and EPR spectroscopy indicated that the two forms represent different redox states of the protein, in line with the results reported on other N2OR[4]. The blue form represents a reduced state (maximum at 640–650 nm), where CuA is mainly (Cu^+-Cu^+), and CuZ is formally described as containing three Cu^+ and one Cu^{2+}. The purple form (maxima at 480, 540, 640 and 800 nm) represents an oxidized state where CuA is in the mixed valence state and CuZ remains unchanged. Both forms can be interconverted. Blue crystals belonging to space group $P6_1$ with cell dimensions a = b = 211 Å, c = 166 Å, α = β = 90°, γ = 120°, were obtained by vapor diffusion technique by mixing 3 μl of N2OR solution (5 mg ml^{-1} in 100 mM Tris pH 7.6) with 3 μl of reservoir solution (18% PEG 4000, 0.1 M BICINE pH 9.5, 0.6 M NaCl, 15% isopropanol,10 mM spermine-4HCl). The absorption spectrum (400–830 nm) of crystals frozen at 100 K showed a dominant band with λ_{max} at 635 nm and a shoulder at 740 nm, closely resembling the absorption spectrum of the reduced blue form in solution (Fig. 4*a*).

Fig. 4 Copper cluster spectrum and electron density map ***a***, Absorption spectrum (400–830 nm) of a crystal frozen at 100 K showing a dominant band with λ_{max} at 635 nm and a shoulder at 740 nm, which are typical of the reduced blue form. ***b***, Stereo view of the $2F_o - F_c$ electron density map (contoured at 1σ) of the CuZ cluster. A red line connects the copper atoms in the cluster; water molecules are colored in red, and the rest of the model is colored according to atom types (C, yellow; N, blue; O, red).

Table 1 Structural statistics

Data collection

	f'' max	f' min	Remote	High resolution
Beamline	BM14	BM14	BM14	ID14-EH4
λ (Å)	1.3751	1.3793	0.8850	0.9790
Resolution (Å)	2.9	2.9	2.9	2.4[1]
R_{sym}[2] (%)	5.4 (23.4)[3]	5.6 (25.0)	6.7 (33.1)	6.9 (35.0)
R_{anom}[4] (%)	5.1 (16.8)	4.8 (18.2)	5.9 (25.0)	5.4 (25.3)
I/σ (I)	7.3 (1.6)	5.3 (1.0)	7.3 (1.6)	5.7 (1.9)
Completeness (%)	100 (100)	100 (100)	97.4 (98.0)	90.7 (85.6)
Anomalous completeness (%)	99.5 (100)	97.7 (100)	85.9 (76.8)	73.3 (59.1)
Redundancy	3.7	3.4	3.1	3.6

Refinement statistics

Resolution (Å)	20–2.4	Mean B factors (Å²): main chain / side chain / solvent	45.4 / 46.42 / 55.08
Total reflections	58,148	R.m.s.d. of B factors: main chain / side chain	1.19 / 1.83
Total atoms/AU (protein / Cu / water)	27,210 / 36/ 1,327	R.m.s.d. of bonds (Å)	0.008
R_{work} / R_{free}[5] (%)	21.6 / 25.0	R.m.s.d. of angles, dihedrals, impropers (°)	2.1, 25.8, 0.8

[1]High-resolution cutoff criteria are $R_{sym} \approx 30\%$ and $(I/\sigma I) \approx 2$ in outer resolution shell.
[2]$R_{sym} = \Sigma|I-<I>|/\Sigma<I>$ where I is intensity and <I> is the average I for all equivalent reflections.
[3]Values in parentheses are for the outer resolution shell.
[4]$R_{anom} = \Sigma|<I^+>-<I^->|/\Sigma(|<I^+>+<I^->|)$ where I^+ and I^- are the intensities of Bijvoet positive and negative reflections, respectively.
[5]Number of reflections in the random test set is 3,007 (1.8%).

Data collection and processing. The X-ray fluorescence from a single crystal of N2OR, frozen at 100 K using 10% ethylene glycol as cryoprotectant, was measured as a function of incident X-ray energy in the vicinity of the copper K-edge. For the MAD data collection on BM14 (ESRF), flash-frozen crystals were used and two energies were chosen near the absorption edge: 9,010 eV (λ = 1.3751 Å) and 8,983 eV (λ = 1.3793 Å), corresponding to the maximum f'' and minimum f', respectively. A third, remote energy was selected at 14,000 eV (λ = 0.885 Å). Data were indexed and integrated with DENZO[24]. The two near-edge data sets were scaled to the remote data set using SCALA[25] and reduced using TRUNCATE[25].

Structure determination. Patterson functions were calculated to 6 Å based on both anomalous and dispersive differences, from which eight sites were identified with SHELX[26]. At this resolution, the sites obtained represented copper clusters, rather than individual copper ions. The coordinates of four additional Cu clusters were obtained by inspection of residual dispersive difference Fourier maps. Phases were calculated from these 12 clusters with MLPHARE[25] and improved by solvent flattening with DM[25]. After iterative rounds of model building using TURBO-FRODO and its option TPPR[27], followed by six-fold, noncrystallographic symmetry averaging with DM[25], the improved map enabled the polypeptide chain to be built from residues 10–581. Preliminary refinement was performed with CNS[28] against a data set collected to 2.4 Å resolution on ID14-EH4 (ESRF, Grenoble) and using bulk solvent correction and NCS restraints. The CuZ center was constructed by successively introducing individual Cu ions into the F_o - F_c sigmaA maps. Iterative rounds of cartesian simulated annealing, followed by anisotropic B-factor refinement and graphical remodeling, enabled the geometry of both copper centers to be improved and eliminated errors elsewhere in the model (Fig. 4*b*). Each monomer consists of residues 10–581, one chloride ion, two calcium ions (identified from their coordination and from difference Fourier maps) and six copper ions; 1,327 solvent molecules were found in the asymmetric unit. The six molecules forming the crystallographic trimer are essentially identical with an r.m.s.d. of 0.2 Å for all Cα atoms. High temperature factors are observed (Table 1). The stereochemistry of the final model was analyzed by PROCHECK[29]; 84% of the residues were found to lie in the most favorable regions of the Ramachandran plot and 15% in additionally allowed regions; two residues per monomer (Lys 286 and Lys 400) were found in forbidden regions, the reason for which is not known.

Coordinates. The coordinates have been deposited with the Protein Data Bank, with accession code 1QNI.

Acknowledgments
We gratefully acknowledge G. Leonard for assistance during data collection at beamline BM14 (ESRF), S. McSweeney for privileged use of beamline ID14-EH4 (ESRF), and T. Ursby (IBS, Grenoble) for assistance in recording the crystal spectra. We also thank W.G. Zumft (Karlsruhe University) for valuable discussions, and P. Marchot, Y. Bourne, J.-M.Claverie and H. van Tilbeurgh for critical reviewing of the manuscript. This work was supported by a EU BIOTECH Structural Biology project.

Correspondence should be addressed to C.C. *email: cambillau@afmb.cnrs-mrs.fr*

Received 29 November, 1999; accepted 31 January, 2000.

1. Dickinson, R.E. & Cicerone, R.J. *Nature* **319**, 109–118 (1986).
2. Reilly, J. *et al. Nature* **401**, 549–555 (1999).
3. Zumft, W.G. & Matsubara, T. *FEBS Lett.* **148**, 107–112 (1982).
4. Zumft, W.G. *Microbiol. Mol. Biol. Rev.* **61**, 533–616 (1997).
5. Matsubara, T. & Zumft, W.G. *Arch. Microbiol.***132**, 322–328 (1982).
6. Scala, D.J. & Kerkhof, L.J. **65**, 1681–1687 (1999).
7. Holm, L., Saraste, M & Wilkström, M. *EMBO J.* **6**, 2819–2823 (1987).
8. Zumft, W.G. *et al. Eur. J. Biochem.* **208**, 31–40 (1992).
9. Keightley, J.A. *et al. J. Biol. Chem.* **270**, 20345–20358 (1995).
10. Williams, P.A. *et al. Nature Struct. Biol.* **6**, 509–516 (1999).
11. Farrar, J.A., Thomson, A.J., Cheesman, M.R., Dooley, D.M. & Zumft, W.G. *FEBS Lett.* **294**, 11–15 (1991).
12. Riester, J., Zumft, W.G. & Kroneck, P.M.H. *Eur. J. Biochem.* **178**, 751–762 (1989).
13. Klabunde, T., Eicken, C., Sacchettini, J.C. & Krebs, B. *Nature Struct. Biol.* **5**,1084–1090 (1998).
14. Volbeda, A. & Hol, W.G. *J. Mol. Biol.* **209**, 249–279 (1989).
15. Messerschmidt, A. *et al. J. Mol. Biol.* **224**, 179–205 (1992).
16. Fülöp, V., Moir, J.W.B., Ferguson, S.J. & Hajdu, J. *Cell* **81**, 369–377 (1995).
17. Ito, N. *et al. Nature* **350**, 87–90 (1991).
18. Fülöp, V., Bocskei, Z. & Polga, L. *Cell* **94**, 161–170 (1998).
19. Tsukihara, T. *et al. Science* **272**, 1136–1144 (1996).
20. Iwata, S., Ostermeier, C., Ludwig, B. & Michel, H. *Nature* **376**, 660–669 (1995).
21. Bergdoll, M., Remy, M-H., Cagnon, C., Masson, J-M. & Dumas, P. *Structure* **5**, 391–401 (1997).
22. McGuirl, M., Nelson, L.K., Bollinger, J.A., Chan, Y-K. & Dolley, D.M. *J. Inorg. Biochem.* **70**, 155–169 (1998).
23. Adman, E.T., Godden, J.W. & Turley, S. *J. Biol. Chem.* **270**, 27458–27474 (1995).
24. Otwinowski, Z. & Minor, W. *Methods Enzymol.* **276**, 307–326 (1997).
25. Collaborative Computational Project, Number 4. CCP4 Suite: programs for protein crystallography. *Acta Crystallogr. D* **50**, 760–763 (1994).
26. Sheldrick, G.M. *Acta Crystallogr. A* **46**, 467–472 (1990).
27. Roussel, A. & Cambillau, C. In *Silicon graphics geometry partners directory.* (ed. Silicon Graphics) 81 (Silicon Graphics, Mountain View, CA; 1991).
28. Brünger, A.T. *et al. Acta Crystallogr. D* **54**, 905–921 (1998).
29. Laskowski, R., MacArthur, M., Moss, D. & Thornton, J. *J. Appl. Crystallogr.* **26**, 91–97 (1993).
30. Kraulis, P.J. *J. Appl. Crystallogr.* **24**, 946–947 (1991).
31. Prudêncio, M. *et al. Biochemistry*, **in the press** (2000).